# Humanoid Robot Balancing

Youngjin Choi[1] and Doik Kim[2]
*[1]Division of Electrical Engineering and Computer Science*
*Hanyang University, Ansan, 426-791,*
*[2] Korea Institute of Science and Technology (KIST), Seoul, 136-791,*
*Rep. of Korea*

## 1. Introduction

There have been many researches about humanoid robot motion control, for example, walking pattern generation (Huang et al, 2001) (Kajita et al, 2002, 2003), walking control (Choi et al, 2006) (Grizzle et al, 2003) (Hirai et al, 1998) (Kajita et al, 2001) (Kim & Oh, 2004), (Lohmeier et al, 2004) (Park, 2001) (Takanishi et al, 1990) (Westervelt et al, 2003), running control (Nagasaki et al, 2004, 2005), balancing control (Kajita et al, 2001) and whole body coordination (Choi et al, 2007) (Kajita et al, 2003) (Sentis & Khatib, 2005) (Goswami & Kallem, 2004) (Harada et al, 2003) (Sugihara & Nakamura, 2002). Especially, the whole body coordination algorithm with good performance becomes a core part in the development of humanoid robot because it is able to offer the enhanced stability and flexibility to the humanoid motion planning. In this chapter, we explain the kinematic resolution method of CoM Jacobian with embedded motion which was suggested in (Choi et al, 2007), actually, which offers the ability of balancing to humanoid robot. For example, if humanoid robot stretches two arms forward, then the position of CoM(center of mass) of humanoid robot moves forward and its ZMP(zero moment point) swings back and forth. In this case, the proposed kinematic resolution method of CoM Jacobian with embedded motion offers the joint configurations of supporting limb(s) calculated automatically to maintain the position of CoM fixed at one point.

Also, a design of balancing controller with good performance becomes another important part in development of humanoid robot. In balancing control, the ZMP control is the most important factor in implementing stable bipedal robot motions. If the ZMP is located in the region of supporting sole, then the robot will not fall down during motions. In order to compensate the error between the desired and actual ZMP, various ZMP control methods have been suggested; for example, direct/indirect ZMP control methods (Choi et al, 2004) (Kajita et al, 2003) and the impedance control (Park, 2001). Despite many references to bipedal balancing control methods, research on the stability of bipedal balancing controllers is still lacking. The exponential stability of periodic walking motion was partially proved for a planar bipedal robot in (Grizzle et al, 2003) (Westervelt et al, 2003). Also, the ISS (disturbance input-to-state stability) of the indirect ZMP controller was proved for the simplified bipedal robot model in (Choi et al, 2004, 2007). In this chapter, we will explain the balancing control method and its ISS proof which were suggested in (Choi et al, 2007). The

suggested method offers the stable balancing control as well as the function of whole body coordination to humanoid robot. Also, the suggested control method includes both the CoM/ZMP trajectory tracking control and CoM/ZMP set-point regulation control based on the kinematic resolution of CoM Jacobian with embedded task motions. Due to the modeling uncertainties and the complexity of the full dynamics of a bipedal walking robot, we will represent the dynamic walking robot as a simple rolling sphere model on a constraint surface. And then the ISS is proved for the simplified model of bipedal robot.

This chapter is organized as follows: section 2 introduces a simplified model for bipedal walking robot, section 3 explains the kinematic resolution method of CoM Jacobian with an embedded task motion, section 4 suggests the balancing controller for humanoid robot and proves its ISS for the simplified bipedal robot model, section 5 shows the experimental results about the stable balancing functions obtained by using the kinematic resolution method of CoM Jacobian with embedded motion, and section 6 concludes the chapter.

## 2. Rolling sphere model

The bipedal walking mechanism is an essential part of humanoid robot. Since humanoid legs have high degrees of freedom for human-like motion, it is difficult to use their full dynamics to design controller and to analyze stability. Therefore, we will simplify the walking related dynamics of bipedal robot as the equation of motion of a point mass concentrated on the position of CoM as shown in Fig. 1.
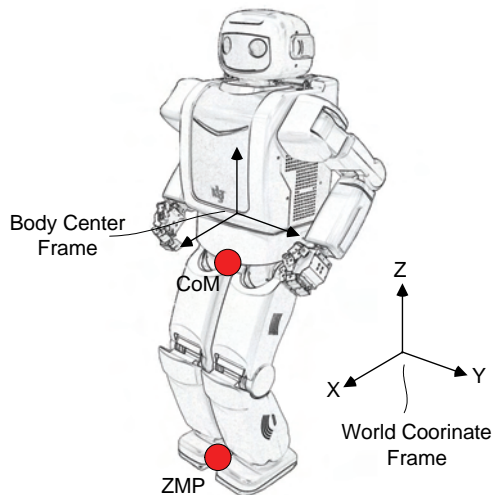


Fig. 1. Humanoid Robot

First, let us assume that the motion of CoM is constrained on the surface, $z = c_z$, then the rolling sphere model with the concentrated point mass $m$ can be obtained as the simplified model for bipedal robot as shown in Fig. 2. In Fig. 2, the motion of the rolling sphere on a massless plate is described by the position of CoM, $c = [c_x, c_y, c_z]^T$, and the ZMP is described by the position on the ground, $p = [p_x, p_y, 0]^T$.
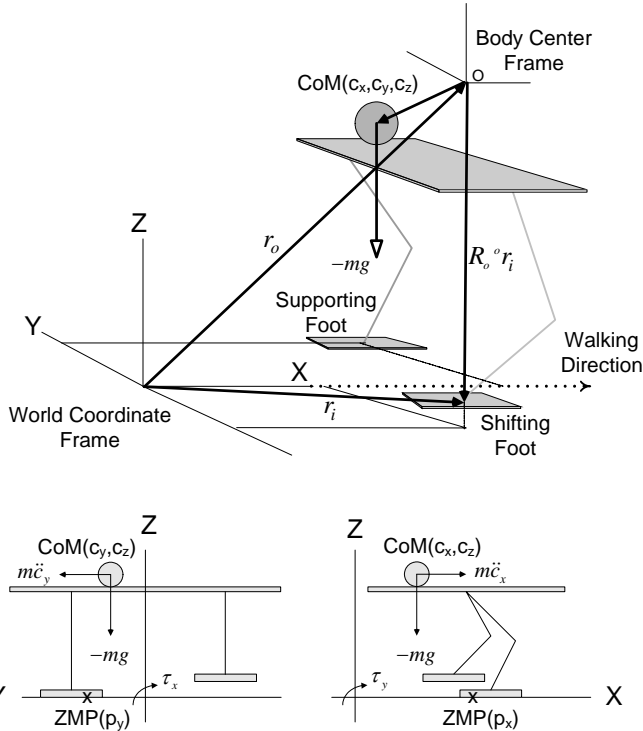
Fig. 2. Rolling Sphere Model for Humanoid Robot

Second, the equations of motion of the rolling sphere (mass $= m$) in Fig. 2 are expressed on the plane $z = c_z$ by:

$$\tau_x = mgc_y - m\ddot{c}_y c_z \tag{1}$$

$$\tau_y = -mgc_x + m\ddot{c}_x c_z \tag{2}$$

$$\tau_z = -m\ddot{c}_x c_y + m\ddot{c}_y c_x$$

where $g$ is the acceleration of gravity, $c_z$ is a height constant of constraint plane and $\tau_i$ is the moment about $i$-th coordinate axis, for $i = x, y, z$. Now, if we introduce the conventional definition of ZMP as following forms to Eq. (1) and (2):

$$p_x = -\frac{\tau_y}{mg}$$

$$p_y = \frac{\tau_x}{mg}$$

then ZMP equations can be obtained as two differential equations:

$$p_x = c_x - \frac{c_z}{g}\ddot{c}_x \tag{3}$$

$$p_y = c_y - \frac{c_z}{g}\ddot{c}_y. \tag{4}$$

Actually, above equations can be easily obtained by finding the position of zero moment on the ground in Fig. 2 like these:

$$\sum M_{p_y} = -mg(p_y - c_y) - (m\ddot{c}_y)c_z = 0$$

$$\sum M_{p_x} = mg(p_x - c_x) + (m\ddot{c}_x)c_z = 0.$$

Also, the state space realization of ZMP equations (3) and (4) can be written as:

$$\frac{d}{dt}\begin{bmatrix} c_i \\ \dot{c}_i \end{bmatrix} = \begin{bmatrix} 0 & 1 \\ \omega_n^2 & 0 \end{bmatrix}\begin{bmatrix} c_i \\ \dot{c}_i \end{bmatrix} + \begin{bmatrix} 0 \\ -\omega_n^2 \end{bmatrix}p_i,$$

for $i = x, y$, where $\omega_n = \sqrt{g/c_z}$ means the natural radian frequency of the simplified biped walking robot system. These state space equations describe the relation between the dynamics of CoM and the ZMP. Above equations will be used to prove the stability of the balancing controller in the following sections.

## 3. Kinematic resolution method for balancing

In this section, we will explain the kinematic resolution method of CoM Jacobian with embedded motion, ultimately for humanoid balancing. Let a robot has $n$ limbs and the first limb be the base limb, for example, $n=4$ for humanoid robot except the neck. The base limb can be any limb but it should be on the ground to support the body. Each limb of a robot is hereafter considered as an independent limb. In general, $i$-th limb has the following relation:

$$^o\dot{x}_i = {}^o J_i \dot{q}_i$$

for $i = 1, 2, \cdots, n$, where ${}^o\dot{x}_i \in \Re^6$ is the velocity of the end point of $i$-th limb, $\dot{q}_i \in \Re^{n_i}$ is the joint velocity of $i$-th limb, ${}^o J_i \in \Re^{6 \times n_i}$ is the usual Jacobian matrix of $i$-th limb, and $n_i$ means the number of active links of $i$-th limb, at least, $n_i \geq 6$ for the limb related with leg. The leading superscript $o$ implies that the elements are represented on the body center coordinate system shown in Fig. 1 and Fig. 2, which is fixed on a humanoid robot.

### 3.1 Compatibility condition
In our case, the body center is floating, and thus the end point motion of $i$-th limb about the world coordinate system is written as follows:

$$\dot{x}_i = X_i^{-1}\dot{x}_o + X_o \, {}^o J_i \dot{q}_i \tag{5}$$

where $\dot{x}_o = [\dot{r}_o^T; \omega_o^T]^T \in \Re^6$ is the velocity of the body center represented on the world coordinate system, and

$$X_i = \begin{bmatrix} I_3 & [R_o \, {}^o r_i \times] \\ 0_3 & I_3 \end{bmatrix} \in \Re^{6 \times 6}$$

is a $(6 \times 6)$ matrix which relates the body center velocity and the $i$-th limb velocity. $I_3$ and $0_3$ are an $(3 \times 3)$ identity and zero matrix, respectively. $R_o \, {}^o r_i$ is the position vector from the body center to the end point of the $i$-th limb represented on the world coordinate frame. $[(\cdot) \times]$ is a skew-symmetric matrix for the cross product. The transformation matrix $X_o$ is

$$X_o = \begin{bmatrix} R_o & 0_3 \\ 0_3 & R_o \end{bmatrix} \in \Re^{6 \times 6}$$

where $R_o \in \Re^{3 \times 3}$ is the orientation of the body center represented on the world coordinate frame, and hereafter, we will use the relation $J_i = X_o \, {}^o J_i$. Also, the concrete proof of Eq. (5) is in appendix 9.1.

All the limbs in a robot should have the same body center velocity, in other words, from Eq. (5), we can see that all the limbs should satisfy the compatibility condition that the body center velocity is the same, and thus, $i$-th limb and $j$-th limb should satisfy the following relation:

$$X_i(\dot{x}_i - J_i \dot{q}_i) = X_j(\dot{x}_j - J_j \dot{q}_j). \tag{6}$$

From Eq. (6), the joint velocity of any limb can be represented by the joint velocity of the base limb and Cartesian motions of limbs. Actually, the base limb should be chosen to be the support leg in single support phase or one of both legs in double support phase. Let us express the base limb with the subscript 1, then the joint velocity of $i$-th limb is expressed as:

$$\dot{q}_i = J_i^+ \dot{x}_i - J_i^+ X_{i1}(\dot{x}_1 - J_1 \dot{q}_1), \tag{7}$$

for $i = 2, \cdots, n$, where $J_i^+$ means the Moore-Penrose pseudoinverse of $J_i$ and

$$X_{i1} = X_i^{-1} X_1 = \begin{bmatrix} I_3 & [R_o({}^o r_1 - {}^o r_i) \times] \\ 0_3 & I_3 \end{bmatrix}.$$

Note that if a limb is a redundant system, any null space optimization scheme can be added in Eq. (7). With the compatibility condition of Eq. (6), the inverse kinematics of humanoid robot can be solved by using the information of base limb like Eq. (7), not by using the information of body center like Eq. (5).

### 3.2 CoM Jacobian with fully specified embedded motions

Now, let us rewrite the conventional CoM Jacobian suggested in (Sugihara & Nakamura, 2002) as follows:

$$\dot{c} = \dot{r}_o + \omega_o \times (c - r_o) + \sum_{i=1}^{n} R_o {}^o J_{c_i} \dot{q}_i. \tag{8}$$

where $n$ is the number of limbs, $c$ is the position vector of CoM represented on the world coordinate system, namely, $c = [c_x, c_y, c_z]^T$ , ${}^o J_{c_i} \in \Re^{3 \times n_i}$ means CoM Jacobian matrix of $i$-th limb represented on the body center coordinate frame, and hereafter, we will use the relation $J_{c_i} = R_o {}^o J_{c_i}$ . Also, the concrete proof of Eq. (8) is in appendix 9.2.
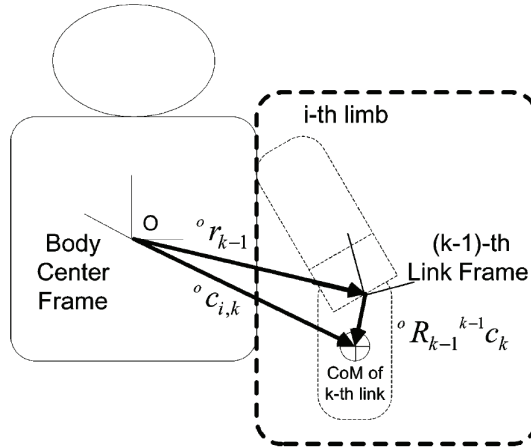


Fig. 3. Position of CoM of the k-th link in i-th limb

**Remark 1** *The CoM Jacobian matrix of i-th limb represented on the body center frame is expressed by*

$$^o J_{c_i} = \sum_{k=1}^{n_i} \mu_{i,k} \frac{\partial {}^o c_{i,k}}{\partial q_i}, \tag{9}$$

*where* ${}^o c_{i,k} \in \Re^3$ *means the position vector of center of mass of k-th link in i-th limb represented on the body center frame as shown in Fig. 3 and the mass influence coefficient of k-th link in i-th limb is defined as follow:*

$$\mu_{i,k} = \frac{m_{i,k}}{\sum_{i=1}^{n} \sum_{k=1}^{n_i} m_{i,k}}, \tag{10}$$

*where* $m_{i,k}$ *is the mass of k-th link in i-th limb. Also, the systematic derivation of CoM Jacobian matrix of Eq. (9) is in appendix 9.3.*

The motion of body center frame can be obtained by using Eq. (5) for the base limb as follows:

$$\dot{x}_o = X_1 \{ \dot{x}_1 - J_1 \dot{q}_1 \}$$

$$\begin{bmatrix} \dot{r}_o \\ \omega_o \end{bmatrix} = \begin{bmatrix} I_3 & [R_o{}^o r_1 \times] \\ 0_3 & I_3 \end{bmatrix} \left\{ \begin{bmatrix} \dot{r}_1 \\ \omega_1 \end{bmatrix} - \begin{bmatrix} J_{v_1} \\ J_{\omega_1} \end{bmatrix} \dot{q}_1 \right\}, \tag{11}$$

where $J_{v_1}$ and $J_{\omega_1}$ are the linear and angular velocity part of the base limb Jacobian $J_1$ expressed on the world coordinate frame, respectively. Now, if Eq. (7) is applied to Eq. (8) for all limbs except the base limb with subscript 1, the CoM motion is rearranged as follows:

$$\dot{c} = \dot{r}_o + \omega_o \times (c - r_o) + J_{c_1} \dot{q}_1 + \sum_{i=2}^{n} J_{c_i} J_i^+ (\dot{x}_i - X_{i1} \dot{x}_1) + \sum_{i=2}^{n} J_{c_i} J_i^+ X_{i1} J_1 \dot{q}_1. \tag{12}$$

Here, if Eq. (11) is applied to Eq. (12), then the CoM motion is only related with the motion of base limb:

$$\dot{c} = \dot{r}_1 + \omega_1 \times r_{c1} - J_{v_1} \dot{q}_1 + r_{c1} \times J_{\omega_1} \dot{q}_1 + J_{c_1} \dot{q}_1 + \sum_{i=2}^{n} J_{c_i} J_i^+ (\dot{x}_i - X_{i1} \dot{x}_1) + \sum_{i=2}^{n} J_{c_i} J_i^+ X_{i1} J_1 \dot{q}_1 \tag{13}$$

where $r_{c1} = c - r_1$. Also, if the base limb has the face contact with the ground (the end-point of base limb represented on world coordinate frame is fixed, $\dot{x}_1 = 0$, namely, $\dot{r}_1 = 0$, $\omega_1 = 0$), then Eq. (13) is simplified as follows:

$$\dot{c} - \sum_{i=2}^{n} J_{c_i} J_i^+ \dot{x}_i = -J_{v_1} \dot{q}_1 + r_{c1} \times J_{\omega_1} \dot{q}_1 + J_{c_1} \dot{q}_1 + \sum_{i=2}^{n} J_{c_i} J_i^+ X_{i1} J_1 \dot{q}_1.$$

Finally, $3 \times n_1$ CoM Jacobian matrix with embedded motions can be rewritten like usual kinematic Jacobian of base limb:

$$\dot{c}_{\text{fsem}} = J_{\text{fsem}} \dot{q}_1, \tag{14}$$

where

$$\dot{c}_{\text{fsem}} = \dot{c} - \sum_{i=2}^{n} J_{c_i} J_i^+ \dot{x}_i, \tag{15}$$

$$J_{\text{fsem}} = -J_{v_1} + r_{c1} \times J_{\omega_1} + J_{c_1} + \sum_{i=2}^{n} J_{c_i} J_i^+ X_{i1} J_1.$$

Here, if the CoM Jacobian is augmented with the orientation Jacobian of body center ($\omega_o = -J_{\omega_1} q_1$) and all desired Cartesian motions are embedded in Eq. (15), then the desired joint configurations of base limb (support limb) are resolved as follows:

$$\dot{q}_{1,d} = \begin{bmatrix} J_{\text{fsem}} \\ -J_{\omega_1} \end{bmatrix}^+ \begin{bmatrix} \dot{c}_{\text{fsem},d} \\ \omega_{o,d} \end{bmatrix}, \tag{16}$$

where the subscript $d$ means the desired motion and

$$\dot{c}_{\text{fsem},d} = \dot{c}_d - \sum_{i=2}^{n} J_{c_i} J_i^+ \dot{x}_{i,d}. \tag{17}$$

All given desired limb motions, $\dot{x}_{i,d}$ are embedded in the relation of CoM Jacobian, thus the effect of the CoM movement generated by the given limb motion is compensated by the base limb. The CoM motion with fully specified embedded motions, $\dot{c}_{\text{fsem},d}$, consists of two relations: a given desired CoM motion(the first term) and the relative effect of other limbs(the second term). The CoM Jacobian with fully specified embedded motions, $J_{\text{fsem}}$ also consists of three relations: the effect of the body center(the first and the second term), the effect of the base limb(the third term), and the effect of other limbs(the last term).

The CoM Jacobian with fully specified embedded motions $J_{\text{fsem}}$ is a $(3 \times n_1)$ matrix where $n_1$ is the dimension of the base limb, which is smaller than that of the original CoM Jacobian, thus the calculation time can be reduced. After solving Eq. (16), the desired joint motion of the base limb is obtained. The resulting base limb motion makes a humanoid robot balanced automatically during the movement of the all other limbs. With the desired joint motion of base limb, the desired joint motions of all other limbs can be obtained by Eq. (7) as follow:

$$\dot{q}_{i,d} = J_i^+ (\dot{x}_{i,d} + X_{i1} J_1 \dot{q}_{1,d}),$$

for $i = 2, \cdots, n$. The resulting motion follows the given desired motions, regardless of balancing motion by base limb. In other words, the suggested kinematic resolution method of CoM Jacobian with embedded motion offers the WBC(whole body coordination) function to the humanoid robot automatically.

### 3.3 CoM Jacobian with partially specified embedded motion
In some cases, the desired motion of any limb is specified in the joint configuration space. For example, let us consider that the walking motions (for the leg limbs of $i=1,2$) are partially specified in Cartesian space and the other limb motions (for $i=3,4$) in joint space, then the kinematic resolution method of Eq. (14) in the previous section should be slightly modified as follows:

$$\dot{q}_{1,d} = \begin{bmatrix} J_{\text{psem}} \\ -J_{\omega_1} \end{bmatrix}^+ \begin{bmatrix} \dot{c}_{\text{psem},d} \\ \omega_{o,d} \end{bmatrix}, \tag{18}$$

$$\dot{q}_{2,d} = J_2^+ (\dot{x}_{2,d} + X_{21} J_1 \dot{q}_{1,d}) \tag{19}$$

where the CoM desired motion and CoM Jacobian with partially specified embedded motion are expressed by, respectively,

$$\dot{c}_{\text{psem},d} = \dot{c}_d - J_{c_2} J_2^+ \dot{x}_{2,d} - \sum_{i=3}^{n} J_{c_i} \dot{q}_{i,d}, \tag{20}$$

$$J_{\text{psem}} = -J_{v_1} + r_{c1} \times J_{\omega_1} + J_{c_1} + J_{c_2} J_2^+ X_{21} J_1.$$

The walking motion is generally specified as the Cartesian desired motions for dual legs but the motions of other limbs can be specified as either joint or Cartesian desired motion. Also, if we are to implement the robot dancing expressed by desired joint motions, then the desired dancing arm motions as well as desired CoM motion are embedded in the suggested resolution method and then the motion of base limb (support leg) are automatically generated with the function of auto-balancing. This is main advantage of the proposed method.

## 4. Design of balancing controller

Since a humanoid robot is an electro-mechanical system including many electric motors, gears and link mechanisms, there are many disturbances in implementing the desired motions of CoM and ZMP for a real bipedal robot system. To show the robustness of the controller to be suggested against disturbances, we apply the following stability theory to a bipedal robot control system. The control system is said to be disturbance input-to-state stable (ISS) (Choi & Chung, 2004), if there exists a smooth positive definite radially unbounded function $V(e,t)$, a class $K_\infty$ function $\gamma_1$ and a class $K$ function $\gamma_2$ such that the following dissipativity inequality is satisfied:

$$\dot{V} \le -\gamma_1(|e|) + \gamma_2(|\varepsilon|), \tag{21}$$

where $\dot{V}$ represents the total derivative for Lyapunov function, $e$ is the error state vector and $\varepsilon$ is disturbance input vector. In this section, we propose the balancing (posture/walking) controller for bipedal robot systems as shown in Fig. 4.
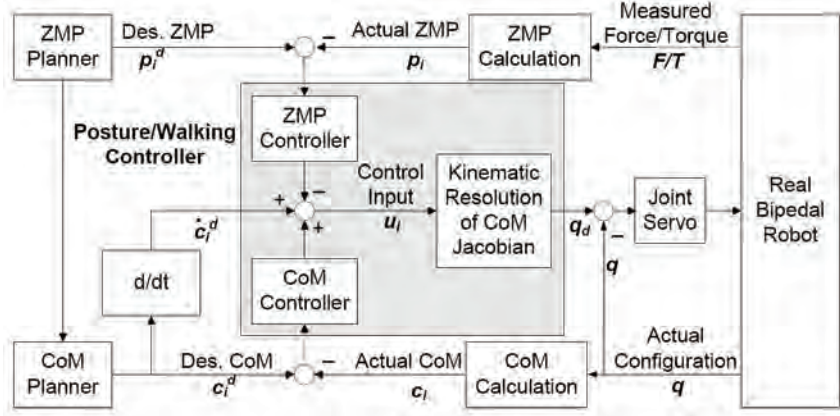


Fig. 4. Balancing Controller for Humanoid Robot

In this figure, first, the ZMP Planer and CoM Planer generate the desired trajectories satisfying the following differential equation:

$$p_{i,d} = c_{i,d} - 1/\omega_n^2 \ddot{c}_{i,d} \quad for \quad i = x, y. \tag{22}$$

Second, the simplified model for the real bipedal walking robot has the following dynamics:

$$\dot{c}_i = u_i + \varepsilon_i \tag{23}$$

$$p_i = c_i - 1/\omega_n^2 \ddot{c}_i \quad for \quad i = x, y$$

where $\varepsilon_i$ is the disturbance input produced by actual control error, $u_i$ is the control input, $c_i$ and $p_i$ are the actual positions of CoM and ZMP measured from the real bipedal robot, respectively. Actually, the real bipedal robot offers the ZMP information from force/torque sensors attached to the ankles of humanoid and the CoM information from the encoder data attached to the motor driving axes, respectively, as shown in Fig. 4. Here, we assume that the disturbance produced by control error is bounded and its differentiation is also bounded, namely, $|\varepsilon_i| < a$ and $|\dot{\varepsilon}_i| < b$ with any positive constants $a$ and $b$. Also, we should notice that the control error always exists in real robot systems and its magnitude depends on the performance of embedded local joint servos. The following theorem proves the stability of the balancing controller to be suggested for the simplified bipedal robot model.

**Theorem 1** *Let us define the ZMP and CoM error for the simplified bipedal robot control system (23) as follows:*

$$e_{p,i} = p_{i,d} - p_i$$

$$e_{c,i} = c_{i,d} - c_i \quad for \quad i = x, y.$$

*If the balancing control input $u_i$ in Fig. 4 has the following form:*

$$u_i = \dot{c}_i^d - k_{p,i} e_{p,i} + k_{c,i} e_{c,i} \tag{24}$$

*under the following gain conditions:*

$$k_{c,i} > \omega_n \quad and \quad 0 < k_{p,i} < \left( \frac{\omega_n^2 - \beta^2}{\omega_n} - \gamma^2 \right) \tag{25}$$

*with any positive constants satisfying the following conditions:*

$$\beta < \omega_n \quad and \quad \gamma < \sqrt{\frac{\omega_n^2 - \beta^2}{\omega_n}},$$

*then the balancing controller gives the disturbance input( $\varepsilon_i, \dot{\varepsilon}_i$ )-to-state( $e_{p,i}, e_{c,i}$ ) stability (ISS) to a simplified bipedal robot, where, the $k_{p,i}$ is the proportional gain of ZMP controller and $k_{c,i}$ is that of CoM controller in Fig. 4.*

*Proof.* First, we get the error dynamics from Eq. (22) and (23) as follows:

$$\ddot{e}_{c,i} = \omega_n^2 (e_{c,i} - e_{p,i}). \tag{26}$$

Second, another error dynamics is obtained by using Eq. (23) and (24) as follows:

$$k_{p,i} e_{p,i} = \dot{e}_{c,i} + k_{c,i} e_{c,i} + \varepsilon_i, \tag{27}$$

also, this equation can be rearranged for $\dot{e}_c$ :

$$\dot{e}_{c,i} = k_{p,i}e_{p,i} - k_{c,i}e_{c,i} - \varepsilon_i. \tag{28}$$

Third, by differentiating the equation (27) and by using equations (26) and (28), we get the following:

$$
\begin{aligned}
\dot{e}_{p,i} &= 1/k_{p,i}\left(\ddot{e}_{c,i} + k_{c,i}\dot{e}_{c,i} + \dot{\varepsilon}_i\right) \\
&= \omega_n^2/k_{p,i}(e_{c,i} - e_{p,i}) + k_{c,i}/k_{p,i}(k_{p,i}e_{p,i} - k_{c,i}e_{c,i} - \varepsilon_i) + (1/k_{p,i})\dot{\varepsilon}_i \\
&= \left(\frac{\omega_n^2 - k_{c,i}^2}{k_{p,i}}\right)e_{c,i} - \left(\frac{\omega_n^2 - k_{p,i}k_{c,i}}{k_{p,i}}\right)e_{p,i} + \frac{1}{k_{p,i}}(\dot{\varepsilon}_i - k_{c,i}\varepsilon_i).
\end{aligned}
\tag{29}
$$

Fourth, let us consider the following Lyapunov function:

$$V(e_{c,i}, e_{p,i}) = \frac{1}{2}\left[(k_{c,i}^2 - \omega_n^2)e_{c,i}^2 + k_{p,i}^2 e_{p,i}^2\right], \tag{30}$$

where $V(e_c, e_p)$ is the positive definite function for $k_{p,i} > 0$ and $k_{c,i} > \omega_n$, except $e_{c,i} = 0$ and $e_{p,i} = 0$. Now, let us differentiate the above Lyapunov function

$$
\begin{aligned}
\dot{V} &= (k_{c,i}^2 - \omega_n^2)e_{c,i}\dot{e}_{c,i} + k_{p,i}^2 e_{p,i}\dot{e}_{p,i} \\
&= -k_{c,i}(k_{c,i}^2 - \omega_n^2)e_{c,i}^2 - k_{p,i}(\omega_n^2 - k_{p,i}k_{c,i})e_{p,i}^2 - (k_{c,i}^2 - \omega_n^2)e_{c,i}\varepsilon_i + k_{p,i}e_{p,i}\dot{\varepsilon}_i - k_{p,i}k_{c,i}e_{p,i}\varepsilon_i \\
&= -k_{c,i}(k_{c,i}^2 - \omega_n^2)e_{c,i}^2 - k_{p,i}(\omega_n^2 - k_{p,i}k_{c,i})e_{p,i}^2 + (k_{c,i}^2 - \omega_n^2)\left(\alpha^2 e_{c,i}^2 - \left|\alpha e_{c,i} + \frac{1}{2\alpha}\varepsilon_i\right|^2 + \frac{1}{4\alpha^2}\varepsilon_i^2\right) \\
&\quad + k_{p,i}\left(\beta^2 e_{p,i}^2 - \left|\beta e_{p,i} - \frac{1}{2\beta}\dot{\varepsilon}_i\right|^2 + \frac{1}{4\beta^2}\dot{\varepsilon}_i^2\right) + k_{p,i}k_{c,i}\left(\gamma^2 e_{p,i}^2 - \left|\gamma e_{p,i} + \frac{1}{2\gamma}\varepsilon_i\right|^2 + \frac{1}{4\gamma^2}\varepsilon_i^2\right) \\
&= -(k_{c,i} - \alpha^2)(k_{c,i}^2 - \omega_n^2)e_{c,i}^2 - k_{p,i}[\omega_n^2 - (k_{p,i} + \gamma^2)k_{c,i} - \beta^2]e_{p,i}^2 \\
&\quad - (k_{c,i}^2 - \omega_n^2)\left|\alpha e_{c,i} + \frac{1}{2\alpha}\varepsilon_i\right|^2 - k_{p,i}\left|\beta e_{p,i} - \frac{1}{2\beta}\dot{\varepsilon}_i\right|^2 - k_{p,i}k_{c,i}\left|\gamma e_{p,i} + \frac{1}{2\gamma}\varepsilon_i\right|^2 \\
&\quad + \left[\frac{(k_{c,i}^2 - \omega_n^2)}{4\alpha^2} + \frac{k_{p,i}k_{c,i}}{4\gamma^2}\right]\varepsilon_i^2 + \frac{k_{p,i}}{4\beta^2}\dot{\varepsilon}_i^2
\end{aligned}
$$

Therefore,

$$
\begin{aligned}
\dot{V} &\leq -(k_{c,i} - \alpha^2)(k_{c,i}^2 - \omega_n^2)e_{c,i}^2 - k_{p,i}[\omega_n^2 - (k_{p,i} + \gamma^2)k_{c,i} - \beta^2]e_{p,i}^2 \\
&\quad + \left[\frac{(k_{c,i}^2 - \omega_n^2)}{4\alpha^2} + \frac{k_{p,i}k_{c,i}}{4\gamma^2}\right]\varepsilon_i^2 + \frac{k_{p,i}}{4\beta^2}\dot{\varepsilon}_i^2
\end{aligned}
\tag{31}
$$

where $e_{c,i}^2$ term is negative definite with any positive constant satisfying $\alpha < \sqrt{\omega_n}$ and $e_{p,i}^2$ term is negative definite under the given conditions (25). Here, since the inequality (31) follows the ISS property (21), we concludes that the proposed balancing controller gives the disturbance input($\varepsilon_i, \dot{\varepsilon}_i$)-to-state($e_{p,i}, e_{c,i}$) stability (ISS) to the simplified control system model of bipedal robot. $\square$

The balancing control input $u_i$ suggested in above Theorem 1 is applied to the term $\dot{c}_d$ in Eq. (17) or Eq. (20). In other words, two equations (17) and (20) should be modified to include the balancing controller (24) to compensate the CoM/ZMP errors as follows:

$$\dot{c}_{\text{fsem},d} = (\dot{c}_d - k_p\,e_p + k_c\,e_c) - \sum_{i=2}^{n} J_{c_i} J_i^+ \dot{x}_{i,d} \tag{32}$$

$$\dot{c}_{\text{psem},d} = (\dot{c}_d - k_p\,e_p + k_c\,e_c) - J_{c_2} J_2^+ \dot{x}_{2,d} - \sum_{i=3}^{n} J_{c_i} \dot{q}_{i,d} \tag{33}$$

where $k_p$ and $k_c$ imply the diagonal matrices with the corresponding $k_{p,i}$ and $k_{c,i}$ elements, respectively, and $e_p$ and $e_c$ imply the corresponding vectors with $e_{p,i}$ and $e_{c,i}$ elements, respectively. Also, in order to obtain the desired joint driving velocity, the kinematic resolution method of Eq. (16) or Eq. (18) suggested in previous section should be applied to the real bipedal robot.

**Remark 2** *Note that the ZMP controller in above theorem has the negative feedback differently from the conventional controller. Also, for practical use, the gain conditions of balancing controller can be simply rewritten without arbitrary positive constants $\beta$ and $\gamma$ as follows:*

$$k_{c,i} > \omega_n \quad and \quad 0 < k_{p,i} < \omega_n \quad for\ i = x, y,$$

*because the stability proof is very conservative in above theorem.*

The suggested balancing control method can be divided as the kinematic resolution and closed-loop kinematic control of CoM Jacobian with embedded motion. First, the proposed kinematic resolution method has main advantage such that it offers the whole body coordination function such as balance control to humanoid robot automatically. Second, the proposed closed-loop kinematic control method offers the stability and robustness to humanoid motion control system against unknown disturbances. For arbitrary given arm motions such as dancing, the partially specified embedded CoM motion term $\dot{c}_{\text{psem},d}$ is automatically changed with the desired arm motions ($\dot{q}_{3,d}$ and $\dot{q}_{4,d}$) in Eq. (33), and then both desired leg motions ($\dot{q}_{1,d}$ and $\dot{q}_{2,d}$) are generated by using the equations (18) and (19).

Like this, the suggested kinematic resolution method offers the whole body coordination function such as balance control to humanoid robot automatically.

## 5. Experimental results

In this section, we show the performance of proposed kinematic resolution method and the robustness of balancing controller through experiments for humanoid robot `Mahru I' developed by KIST. Its Denavit-Hartenberg parameters for kinematics and centroid/mass data for CoM kinematics are in Table 1. These data are utilized to resolve the CoM Jacobian with embedded motions kinematically.

First, in order to show the automatic balancing (or the function of WBC) by the kinematic resolution method developed in section 3, we implemented the dancing motion of humanoid robot. The desired dancing arm motions shown in Fig. 5 are applied to the dual

| Left Leg | $\alpha$ (rad) | a (m) | d (m) | $\theta$ (rad) | Centroid($\sigma_x,\sigma_y,\sigma_z$)(m) | Mass(kg) |
|---|---|---|---|---|---|---|
| LL0 | 0 | 0.09 | -0.146 | $\pi/2$ | (0.0,0.031,-0.0338) | 2.067 |
| 1 | $\pi/2$ | 0 | 0 | 0 | (0.0295,0.0,-0.0015) | 1.8206 |
| 2 | $\pi/2$ | 0 | 0 | $-\pi/2$ | (0.2249,0.0187,-0.0156) | 3.3586 |
| 3 | 0 | 0.31 | 0 | 0 | (0.1451,0.0285,-0.0026) | 2.2238 |
| 4 | 0 | 0.31 | 0 | 0 | (0.0,-0.0257,-0.0143) | 2.6922 |
| 5 | $-\pi/2$ | 0 | 0 | 0 | (0.0951,0.0047,0.0083) | 1.9091 |
| 6 | 0 | 0.103 | 0 | 0 | x | x |
| Right Leg | | | | | | |
| RL0 | 0 | -0.09 | -0.146 | $\pi/2$ | (0.0,0.031,-0.0338) | 2.067 |
| 1 | $\pi/2$ | 0 | 0 | 0 | (-0.0295,0.0,-0.0015) | 1.8206 |
| 2 | $\pi/2$ | 0 | 0 | $-\pi/2$ | (0.2249,0.0187,0.0156) | 3.3586 |
| 3 | 0 | 0.31 | 0 | 0 | (0.1451,0.0285,0.0026) | 2.2238 |
| 4 | 0 | 0.31 | 0 | 0 | (0.0,-0.0257,0.0143) | 2.6922 |
| 5 | $-\pi/2$ | 0 | 0 | 0 | (0.0951,-0.0047,0.0083) | 1.9091 |
| 6 | 0 | 0.103 | 0 | 0 | x | x |
| Left Arm | | | | | | |
| LA0 | 0 | 0 | 0 | 0 | (0.0278,0.0,-0.051) | 0.823 |
| 1 | $-\pi/2$ | 0 | -0.061 | $-\pi/2$ | (0.062,0.000125,-0.0085) | 1.437 |
| 2 | $\pi/2$ | 0 | -0.0055 | $\pi/2$ | (0.00798,-0.00146,0.2) | 0.9 |
| 3 | $-\pi/2$ | 0 | 0.224 | $\pi/2$ | (0.0,-0.0228,0.00739) | 0.11 |
| 4 | $\pi/2$ | 0 | 0 | 0 | (-0.0025,0.000035,0.153) | 0.781 |
| 5 | $-\pi/2$ | 0 | 0.225 | $-\pi/2$ | (0.0,-0.0208,0.017) | 0.053 |
| 6 | 0 | 0.041 | 0 | $-\pi/2$ | x | x |
| Right Arm | | | | | | |
| RA0 | 0 | 0 | 0 | 0 | (0.0278,0.0,0.051) | 0.823 |
| 1 | $-\pi/2$ | 0 | 0.061 | $-\pi/2$ | (0.062,0.000125,-0.0085) | 1.437 |
| 2 | $\pi/2$ | 0 | -0.0055 | $\pi/2$ | (-0.00798,-0.00146,0.2) | 0.9 |
| 3 | $-\pi/2$ | 0 | 0.224 | $\pi/2$ | (0.0,-0.0228,-0.00739) | 0.11 |
| 4 | $\pi/2$ | 0 | 0 | 0 | (-0.0025,0.000035,0.153) | 0.781 |
| 5 | $-\pi/2$ | 0 | 0.225 | $-\pi/2$ | (0.0,-0.0208,0.017) | 0.053 |
| 6 | 0 | 0.041 | 0 | $-\pi/2$ | x | x |
| Head | | | | | | |
| H0 | 0 | 0.04 | 0.47 | 0 | (0.0,0.0,0.0) | 0.5 |
| 1 | $-\pi/2$ | 0 | 0 | 0 | (0.0,0.0,0.0) | 0.5 |
| 2 | 0 | 0 | 0 | 0 | x | x |
| Pelvis | x | x | x | x | (-0.056,0.0,-0.0173) | 4.6341 |
| Waist | x | x | x | x | (0.0,0.0,0.17) | 25.7 |

Table 1. The DH parameters, centroid and mass data of KIST humanoid `Mahru I'

arms, and then the motions of support left/right legs are generated as shown in Fig. 6 by the suggested kinematic resolution method of CoM Jacobian with embedded dancing arm motions. Actually, we utilized the kinematic resolution method of CoM Jacobian with the partially specified embedded motion, namely, Eq. (18) and Eq. (19). The initial positions of CoM are $c_x = 0.034[m]$, $c_y = 0.0[m]$, $c_z = 0.687[m]$, respectively. The experimental results show the good performance of proposed method. Though the joint configurations of dual arms are rapidly changed with the dancing motion given as shown in Fig. 5, the position of CoM is not nearly changed at the initial position as shown in Fig. 6. The joint configurations of both legs are automatically generated as shown in Fig. 7 to maintain the CoM position constantly. Also, we can see in Fig. 8 that the ZMP has the small changes within the bounds of $\pm 0.01[m]$ approximately. As a result, we could succeed in implementing the fast dancing motion stably thanks to the developed kinematic resolution method of CoM Jacobian with embedded (dancing) motion.
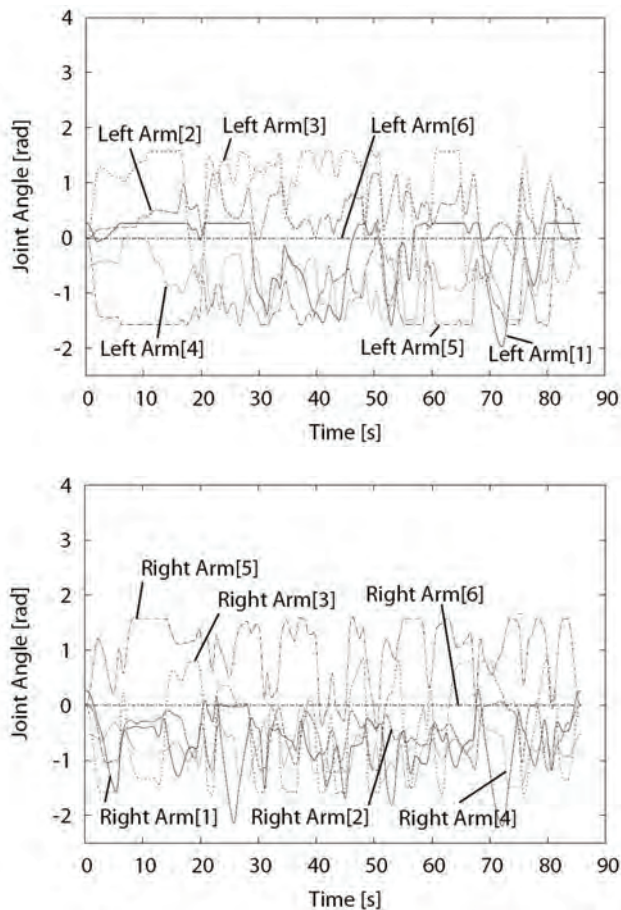


Fig. 5. Desired Joint Trajectories of Left and Right Arms while Dancing
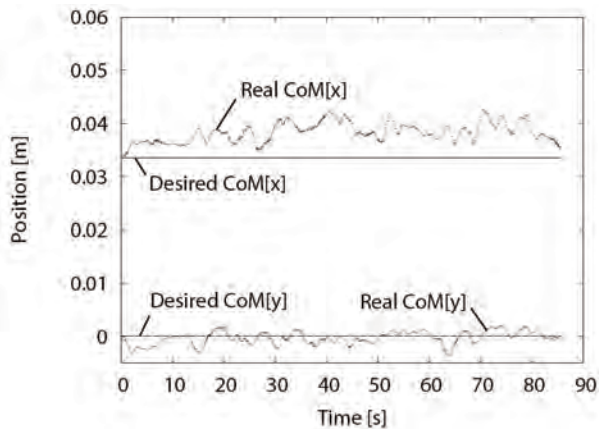
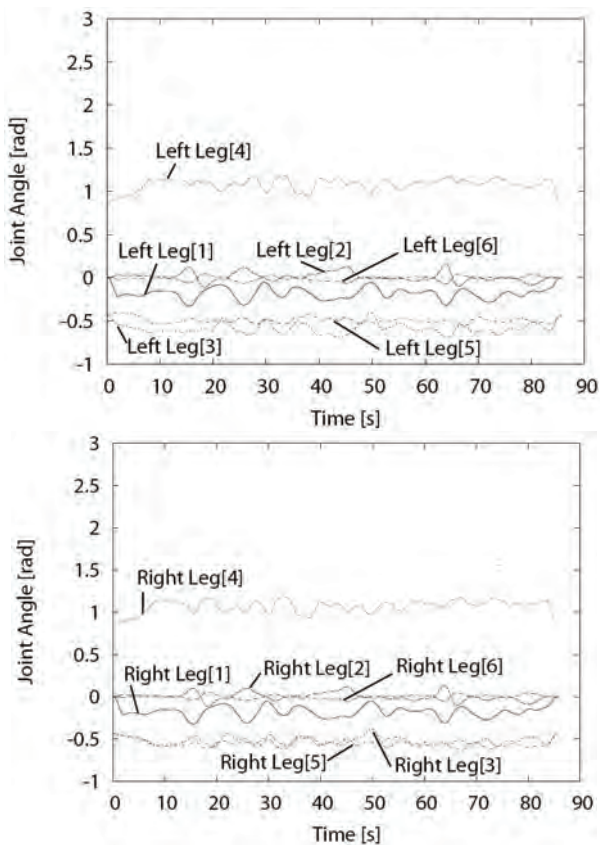Fig. 6. Experimental Result: Actual CoM Trajectories while Dancing



Fig. 7. Experimental Result: Actual Joint Trajectories of Left and Right Legs generated by the developed Kinematic Resolution Method while Dancing
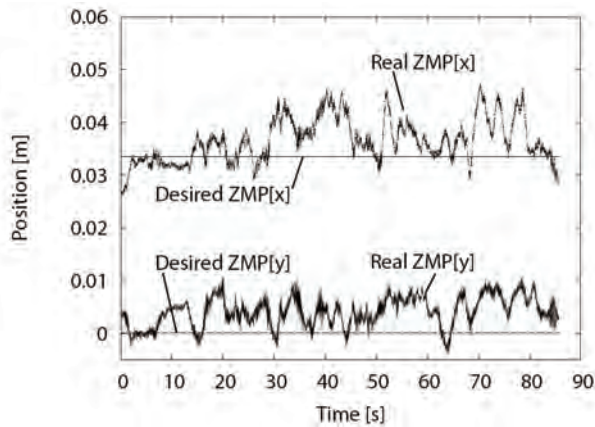
Fig. 8. Experimental Result: Actual ZMP Trajectories while Dancing

 Second, in order to show the performance of the suggested balancing controller of Eq. (33) against external disturbances, we realized the corresponding experiments only for both legs as shown in Fig. 9. In experiment, if we push the robot forward or pull it backward, then the ZMP errors are caused and these ZMP errors give rise to the balancing controller input of Eq. (33) and then the balancing control input is resolved using the suggested resolution method of Eq. (18) and Eq. (19). Hence, the robot was able to recover the original posture as shown in Fig. 9. These results demonstrate the robustness and performance of proposed balancing controller.
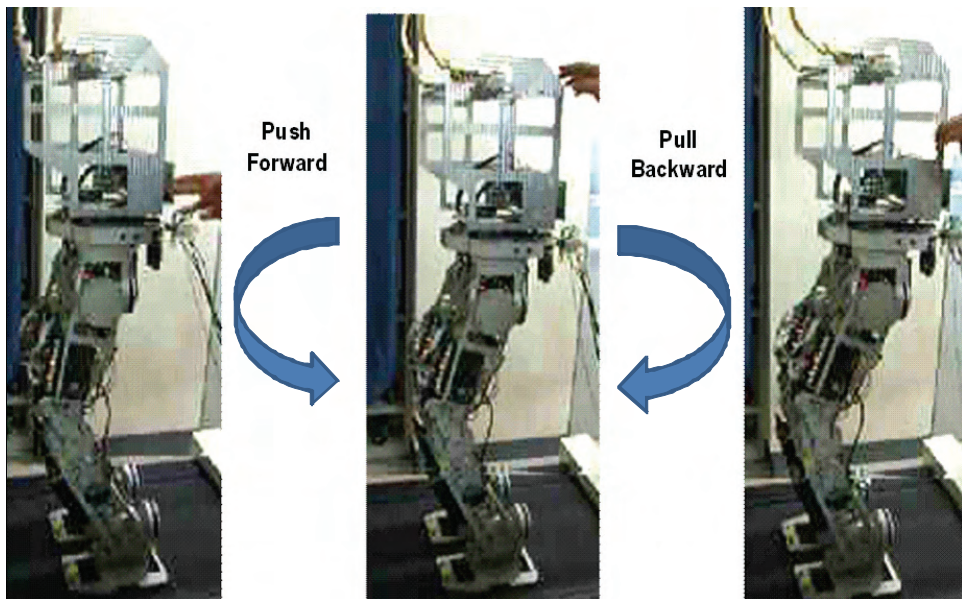


Fig. 9. Experimental Result: Performance of Balancing Controller

## 6. Concluding remarks

In this chapter, the kinematic resolution method of CoM Jacobian with embedded task motion and the balancing control method were proposed for humanoid robot. The proposed kinematic resolution method with CoM Jacobian offers the whole body coordination function to the humanoid robot automatically. Also, the disturbance input-to-state stability (ISS) of the proposed balancing controller was proved to show the robustness against disturbances. Finally, we showed the effectiveness of the proposed methods through experiments.

## 7. References

Choi, Y.; Kim, D.; Oh, Y. & You, B-J. (2007). Posture/Walking Control of Humanoid Robot based on the Kinematic Resolution of CoM Jacobian with Embedded Motion, *IEEE Trans. on Robotics*, Vol 23, No. 6, pp. 1285-1293.

Choi, Y.; Kim, D. & You B-J. (2006) On the Walking Control for Humanoid Robot based on the Kinematic Resolution of CoM Jacobian with Embedded Motion, *IEEE Int. Conf. on Robotics and Automation*, pp, 2655-2660.

Choi, Y.; You, B-J. & Oh, S.R. (2004). On the stability of indirect ZMP controller for biped robot systems, *Proc. of IEEE/RSJ Int. Conf. on Intelligent Robots and Systems*, pp. 1966–1971.

Choi, Y. & Chung, W-K.; (2004). *PID Trajectory Tracking Control for Mechanical Systems*, ser. Lecture Notes in Control and Information Sciences (LNCIS). Springer, Vol. 298, New York.

Huang, Q.; Yokoi, K.; Kajita, S.; Kaneko, K.; Arai, H.; Koyachi, N. & Tanie, K. (2001). Planning walking patterns for a biped robot, *IEEE Trans. on Robotics and Automation*, Vol. 17, No. 3, pp. 280–289.

Grizzle, J.W.; Westervelt, E.R. & Wit, C.C. (2003). Event-based PI control of a underactuated biped walker, *Proc., 42nd IEEE Conf. on Decision and Control*, pp. 3091–3096.

Hirai, K.; Hirose, M.; Haikawa, Y. & Takenaka, T. (1998). The development of Honda humanoid robot, *Proc. of IEEE Int. Conf. on Robotics and Automation*, pp. 1321–1326.

Kajita, S.; Saigo, M. & Tanie, K. (2001). Balancing a humanoid robot using backdrive concerned torque control and direct angular momentum feedback, *Proc. of IEEE Int. Conf. on Robotics and Automation*, pp. 3376–3382.

Kajita, S.; Kanehiro, F.; Kaneko, K.; Fujiwara, K.; Yokoi, K. & Hirukawa, H. (2002). A realtime pattern generator for biped walking, *Proc. of IEEE Int. Conf. on Robotics and Automation*, pp. 31–37.

Kajita, S.; Kanehiro, F.; Kaneko, K.; Fujiwara, K.; Harada, K.; Yokoi, K. & Hirukawa, H. (2003). Biped walking pattern generation by using preview control of zero-moment point, *Proc. of IEEE Int. Conf. on Robotics and Automation*, pp. 1620–1626.

Kajita, S.; Kanehiro, F.; Kaneko, K.; Fujiwara, K.; Harada, K.; Yokoi, K. & Hirukawa, H.; (2003). Resolved momentum control : Humanoid motion planning based on the linear and angular momentum, *Proc. of IEEE Int. Conf. on Robotics and Automation*, pp. 1644–1650.

Kim, J-H. & Oh, J-H. (2004). Walking control of the humanoid platform KHR-1 based on torque feedback control, *Proc. of IEEE Int. Conf. on Robotics and Automation*, pp. 623–628.

Lohmeier, S.; Loffler, K.; Gienger, M.; Ulbrich, H. & Pfeiffer, F.; (2004). Computer system and control of biped "Johnnie", *Proc. of IEEE Int. Conf. on Robotics and Automation*, pp. 4222–4227.

Park, J-H. (2001). Impedance control for biped robot locomotion, *IEEE Trans. on Robotics and Automation*, Vol. 17, No. 6, pp. 870–882.

Takanishi, A.; Lim, H.; Tsuda, M. & Kato, I.; (1990). Realization of dynamic biped walking stabilized by trunk motion on a sagittally uneven surface, *Proc. of IEEE/RSJ Int. Conf. on Intelligent Robots and Systems*, pp. 323– 330.

Westervelt, E-R.; Grizzle, J-W. & Koditschek, D-E.; (2003). Hybrid zero dynamics of planar biped walkers, *IEEE Trans. on Automatic Control*, Vol. 48, No. 1, pp. 42–56.

Nagasaka, K.; Kuroki, Y.; Suzuki, S.; Itoh, Y. & Yamaguchi, J.; (2004). Integrated motion control for walking, jumping and running on a small bipedal entertainment robot, *Proc. of IEEE Int. Conf. on Robotics and Automation*, pp. 3189–3194.

Nagasaki, T.; Kajita, S.; Yokoi, K.; Kaneko, K. & Tanie, K.; (2003). Running pattern generation and its evaluation using a realistic humanoid model, *Proc. of IEEE Int. Conf. on Robotics and Automation*, pp. 1336–1342.

Sentis, L. & Khatib, O.; (2005). Synthesis of whole-body behaviors through hierarchical control of behavioral primitives, *International Journal of Humanoid Robotics*, Vol. 2, No. 4, pp. 505–518.

Goswami, A. & Kallem, V.; (2004). Rate of change of angular momentum and balance maintenance of biped robots, *Proc. of IEEE Int. Conf. on Robotics and Automation*, pp. 3785–3790.

Harada, K.; Kajita, S.; Kaneko, K. & Hirukawa, H.; (2003). ZMP analysis for arm/leg coordination, *Proc. of IEEE Int. Conf. on Robotics and Automation*, pp. 75–81.

Sugihara, T. & Nakamura, Y.; (2002). Whole-body cooperative balancing of humanoid robot uisng COG Jacobian, *Proc. of IEEE/RSJ Int. Conf. on Intelligent Robots and Systems*, pp. 2575–2580.

## 8. Acknowledgement

## 9. Appendix

### 9.1 Proof of Eq. (5)

In Fig. 1, the position of $i$-th limb represented on the world coordinate is given by

$$r_i = r_o + R_o {}^o r_i$$

where $R_o$ is the rotation matrix of body center frame with respect to world coordinate frame. Let's differentiate above equation, then

$$\dot{r}_i = \dot{r}_o + \dot{R}_o {}^o r_i + R_o {}^o \dot{r}_i \quad \leftarrow \dot{R}_o = [\omega_o \times] R_o$$

$$\dot{r}_i = \dot{r}_o + [\omega_o \times] R_o {}^o r_i + R_o {}^o \dot{r}_i \quad \leftarrow [a \times] b = -b [\times a]$$

$$\dot{r}_i = \dot{r}_o - [R_o {}^o r_i \times] \omega_o + R_o {}^o \dot{r}_i$$

in which,

$$[a\times] = \begin{bmatrix} 0 & -a_z & a_y \\ a_z & 0 & -a_x \\ -a_y & a_x & 0 \end{bmatrix}$$

Now, if we include the angular velocity, then the total velocity of $i$-th limb motion represented on the world coordinate can be obtained as follows:

$$\dot{r}_i = \dot{r}_o - [R_o{}^o r_i \times]\omega_o + R_o{}^o \dot{r}_i$$

$$\omega_i = \omega_o + R_o{}^o \omega_i$$

Therefore,

$$\begin{bmatrix} \dot{r}_i \\ \omega_i \end{bmatrix} = \begin{bmatrix} I_3 & -[R_o{}^o r_i \times] \\ 0_3 & I_3 \end{bmatrix}\begin{bmatrix} \dot{r}_o \\ \omega_o \end{bmatrix} + \begin{bmatrix} R_o & 0_3 \\ 0_3 & R_o \end{bmatrix}\begin{bmatrix} {}^o \dot{r}_i \\ {}^o \omega_i \end{bmatrix}$$

in short,

$$\therefore \quad \dot{x}_i = X_i^{-1}\dot{x}_o + X_o{}^o J_i \dot{q}_i$$

### 9.2 Proof of Eq. (8)

In Fig. 1, the position of CoM represented on the world coordinate is given by

$$c = r_o + \sum_{i=1}^{n} R_o{}^o c_i$$

Let us differentiate above equation, then

$$\dot{c} = \dot{r}_o + \sum_{i=1}^{n}(\dot{R}_o{}^o c_i + R_o{}^o \dot{c}_i)$$

$$\dot{c} = \dot{r}_o + \omega_o \times \sum_{i=1}^{n} R_o{}^o c_i + \sum_{i=1}^{n} R_o{}^o \dot{c}_i$$

$$\dot{c} = \dot{r}_o + \omega_o \times (c - r_o) + \sum_{i=1}^{n} R_o{}^o \dot{c}_i \quad \leftarrow {}^o \dot{c}_i = {}^o J_{ci} \dot{q}_i$$

$$\therefore \quad \dot{c} = \dot{r}_o + \omega_o \times (c - r_o) + \sum_{i=1}^{n} R_o{}^o J_{ci} \dot{q}_i$$

### 9.3 Derivation of CoM jacobian of $i$-h limb: ${}^o J_{c_i}$

The CoM position of $k$-th link in $i$-th limb represented on the body center frame is given by

$$^{o}c_{i,k} = {}^{o}r_{k-1} + {}^{o}R_{k-1}{}^{k-1}c_{k}$$

where $^{o}r_{k-1}$ and $^{o}R_{k-1}$ mean the position and rotation matrix of (k-1)-th link frame in i-th limb represented on the body center frame, respectively, and

$$^{k-1}c_{k} = R_{z}(q_{k})\sigma_{k} = \begin{bmatrix} \cos(q_{k}) & -\sin(q_{k}) & 0 \\ \sin(q_{k}) & \cos(q_{k}) & 0 \\ 0 & 0 & 1 \end{bmatrix} \begin{bmatrix} \sigma_{k,x} \\ \sigma_{k,y} \\ \sigma_{k,z} \end{bmatrix}$$

in which $R_{z}(q_{k})$ is the z-directional rotation matrix about k-th link driving axis and $\sigma_{k}$ means the constant centroid position of k-th link with respect to (k-1)-th frame, this should be obtained from the design procedures of robot similarly to the Denavit-Hartenberg parameters. Let us differentiate and rearrange above equation like this:

$$\begin{aligned} ^{o}\dot{c}_{i,k} &= {}^{o}\dot{r}_{k-1} + {}^{o}\dot{R}_{k-1}{}^{k-1}c_{k} + {}^{o}R_{k-1}{}^{k-1}\dot{c}_{k} \\ &= {}^{o}\dot{r}_{k-1} + {}^{o}\omega_{k-1} \times {}^{o}R_{k-1}{}^{k-1}c_{k} + {}^{o}R_{k-1}({}^{k-1}\omega_{k} \times {}^{k-1}c_{k}) \\ &= {}^{o}\dot{r}_{k-1} + {}^{o}\omega_{k} \times {}^{o}R_{k-1}{}^{k-1}c_{k} \qquad since \ {}^{o}\omega_{k} = {}^{o}\omega_{k-1} + {}^{o}R_{k-1}{}^{k-1}\omega_{k} \\ &= {}^{o}\dot{r}_{k-1} + {}^{o}\omega_{k} \times {}^{o}R_{k-1}R_{z}(q_{k})\sigma_{k}, \end{aligned}$$

in which

$$^{o}\omega_{k} = {}^{o}\omega_{k-1} + \dot{q}_{k}({}^{o}z_{k-1})$$

$$^{o}\dot{r}_{k-1} = {}^{o}\dot{r}_{k-2} + {}^{o}\omega_{k-1} \times ({}^{o}r_{k-1} - {}^{o}r_{k-2}).$$

where $^{o}z_{k-1}$ means the z-direction (or driving axis) vector of (k-1)-th link frame represented on body center frame. For instance, for k=1 (first link of i-th limb),

$$\begin{aligned} ^{o}\dot{c}_{i,1} &= {}^{o}\dot{r}_{0} + {}^{o}\omega_{1} \times {}^{o}R_{0}R_{z}(q_{1})\sigma_{1} \\ &= \dot{q}_{1}[{}^{o}z_{0} \times {}^{o}R_{0}R_{z}(q_{1})\sigma_{1}], \end{aligned}$$

for k=2 (second link of i-th limb),

$$\begin{aligned} ^{o}\dot{c}_{i,2} &= {}^{o}\dot{r}_{1} + {}^{o}\omega_{2} \times {}^{o}R_{1}R_{z}(q_{2})\sigma_{2} \\ &= \dot{q}_{1}[{}^{o}z_{0} \times ({}^{o}r_{1} - {}^{o}r_{0})] + [\dot{q}_{1}({}^{o}z_{0}) + \dot{q}_{2}({}^{o}z_{1})] \times {}^{o}R_{1}R_{z}(q_{2})\sigma_{2} \\ &= \dot{q}_{1}[{}^{o}z_{0} \times ({}^{o}r_{1} - {}^{o}r_{0} + {}^{o}R_{1}R_{z}(q_{2})\sigma_{2})] + \dot{q}_{2}[{}^{o}z_{1} \times {}^{o}R_{1}R_{z}(q_{2})\sigma_{2}] \end{aligned}$$

for k=3 (third link of i-th limb),

$$\begin{aligned} ^{o}\dot{c}_{i,3} &= {}^{o}\dot{r}_{2} + {}^{o}\omega_{3} \times {}^{o}R_{2}R_{z}(q_{3})\sigma_{3} \\ &= \dot{q}_{1}[{}^{o}z_{0} \times ({}^{o}r_{2} - {}^{o}r_{0})] + \dot{q}_{2}[{}^{o}z_{1} \times ({}^{o}r_{2} - {}^{o}r_{1})] + [\dot{q}_{1}({}^{o}z_{0}) + \dot{q}_{2}({}^{o}z_{1}) + \dot{q}_{3}({}^{o}z_{2})] \times {}^{o}R_{2}R_{z}(q_{3})\sigma_{3} \\ &= \dot{q}_{1}[{}^{o}z_{0} \times ({}^{o}r_{2} - {}^{o}r_{0} + {}^{o}R_{2}R_{z}(q_{3})\sigma_{3})] + \dot{q}_{2}[{}^{o}z_{1} \times ({}^{o}r_{2} - {}^{o}r_{1} + {}^{o}R_{2}R_{z}(q_{3})\sigma_{3})] + \dot{q}_{3}[{}^{o}z_{2} \times {}^{o}R_{2}R_{z}(q_{3})\sigma_{3}] \end{aligned}$$

for $k = n_i$ (last link of $i$-th limb),

$$
\begin{aligned}
{}^o\dot{c}_{i,n_i} &= {}^o\dot{r}_{n_i-1} + {}^o\omega_{n_i} \times {}^oR_{n_i-1}R_z(q_{n_i})\sigma_{n_i} \\
&= \dot{q}_1[{}^oz_0 \times ({}^or_{n_i-1} - {}^or_0 + {}^oR_{n_i-1}R_z(q_{n_i})\sigma_{n_i})] + \dot{q}_2[{}^oz_1 \times ({}^or_{n_i-1} - {}^or_1 + {}^oR_{n_i-1}R_z(q_{n_i})\sigma_{n_i})] + \cdots \\
&\quad + \dot{q}_{n_i}[{}^oz_{n_i-1} \times {}^oR_{n_i-1}R_z(q_{n_i})\sigma_{n_i}]
\end{aligned}
$$

The CoM position of $i$-th limb represented on the body center frame is obtained as follow:

$$
{}^oc_i = \sum_{k=1}^{n_i} \mu_{i,k} \, {}^oc_{i,k}
$$

where $\mu_{i,k}$ means the mass influence coefficient of $k$-th link in $i$-th limb defined as Eq. (10). Also, its derivative has the following form:

$$
{}^o\dot{c}_i = \sum_{k=1}^{n_i} \mu_{i,k} \, {}^o\dot{c}_{i,k}
$$

Therefore,

$$
{}^o\dot{c}_i = \begin{bmatrix} j_1, j_2, j_3, \cdots, j_{n_i} \end{bmatrix} \begin{bmatrix} \dot{q}_1 \\ \dot{q}_2 \\ \dot{q}_3 \\ \vdots \\ \dot{q}_{n_i} \end{bmatrix}
$$

where

$$
j_1 = \sum_{k=1}^{n_i} \mu_{i,k} \{ {}^oz_0 \times ({}^or_{k-1} - {}^or_0 + {}^oR_{k-1}R_z(q_k)\sigma_k) \}
$$

$$
j_2 = \sum_{k=2}^{n_i} \mu_{i,k} \{ {}^oz_1 \times ({}^or_{k-1} - {}^or_1 + {}^oR_{k-1}R_z(q_k)\sigma_k) \}
$$

$$
j_3 = \sum_{k=3}^{n_i} \mu_{i,k} \{ {}^oz_2 \times ({}^or_{k-1} - {}^or_2 + {}^oR_{k-1}R_z(q_k)\sigma_k) \}
$$

$$
j_{n_i} = \mu_{i,n_i} \{ {}^oz_{n_i-1} \times ({}^oR_{n_i-1}R_z(q_{n_i})\sigma_{n_i}) \}
$$

In short,

$$
\therefore \quad {}^o\dot{c}_i = {}^oJ_{c_i}\dot{q}_i
$$

In addition, the total CoM position represented on the body center frame is also obtained as follow:

$$\therefore \quad {}^{o}c = \sum_{i=1}^{n} {}^{o}c_{i} = \sum_{i=1}^{n} \sum_{k=1}^{n_i} \mu_{i,k} \, {}^{o}c_{i,k}$$